Journal of Applied Geophysics 82 (2012) 19–29

Contents lists available at SciVerse ScienceDirect

Journal of Applied Geophysics

journal homepage: www.elsevier.com/locate/jappgeo

Re-estimating the epicenter of the 1927 Jericho earthquake using spatial distribution of intensity data

Motti Zohar [a,*,1], Shmuel Marco [b]

[a] Department of Geography and Human Environment, Tel Aviv University, Tel Aviv 69978, Israel
[b] Department of Geophysics and Planetary sciences, Tel Aviv University, Tel Aviv 69978, Israel

ARTICLE INFO

Article history:
Received 11 July 2011
Accepted 8 March 2012
Available online 19 March 2012

Keywords:
Earthquakes
Intensity
Epicenter
Attenuation relation
1927
Dead Sea Fault

ABSTRACT

We present a new approach for re-estimating an epicenter of historical earthquake using the spatial distribution of intensity data. We use macroseismic data related to the 1927 Jericho earthquake since this is the first strong earthquake recorded by modern seismographs and is also well documented by historical evidence and reports. The epicenter is located in two sequential steps: (1) Correction of previously-evaluated seismic intensities in accordance with the local site-attributes: construction quality, topographic slope, groundwater level, and surface geology; (2) Spatial correlation of these intensities with a logarithmic variant of the epicentral distance. The resulted location (approximated to 35.5°/31.8°) is consistent with the seismogram-based location calculated by Avni et al. (2002) and also of Ben Menahem et al. (1976) with a spatial error of 50 km. The proposed method suggests an additional approach to the formers based mainly upon spatial analysis of intensity data.

1. Introduction

The determination of an earthquake's epicenter is important both for understanding the underlying tectonic structure and for assessing seismic hazard for given areas. For modern earthquakes recorded by seismographs, the epicenters are calculated by using seismic networks. However, for strong earthquakes that occurred before the instrumental era, such seismological measurements are not available.

During the last three millennia, historical reports and evidence of destructive earthquakes have accumulated (e.g., Ambraseys, 2009; Ambraseys et al., 1994; Guidoboni and Comastri, 2005; Guidoboni et al., 1994; Sbeinati et al., 2005). These include reports, chronicles, contemporary accounts, drawings, manuscripts, archaeological remains and paleoseismic findings. Although subjective, incomplete and occasionally associated with uncertainties (Ambraseys, 2005; Cecic and Musson, 2004; Karcz and Lom, 1987), they significantly expand the seismological record. Thus, an investigation of these historical records becomes critical in understanding the areal distribution of the seismogenic damage.

Quantification of historical records is commonly addressed by classifying the damage at a given locality into 'seismic intensity', ranging from almost unfelt damage to total destruction. Commonly used intensity scales are the MMI (Modified Mercalli Intensity) (Wood and Neumann, 1931), MSK (Medvedev Sponheuer and Karnik) (Medvedev et al., 1965), the EMS (European Macroseismic Scale) (Grünthal, 1998) and the recently developed INQUA (ESI-2007) scale (Michetti et al., 2004). The determination of source parameters from the intensity data is not trivial; nevertheless, quantification of the damage in terms of seismic intensities is almost the only way so far to resolve historical earthquakes (e.g., Avni, 1999; Avni et al., 2002; Bakun and Wentworth, 1997; Bakun et al., 2003; Feldman and Shapira, 1994; Gasperini et al., 2010; Sirovich, 1996; Sirovich and Pettenati, 2001; Sirovich et al., 2001).

During the last two decades, spatial techniques have been rapidly developed and become a powerful tool for analyzing geographic data (Johnston et al., 2001). Supported by GIS-based tools, they enable management and manipulation of geographic data to conclude spatial insights (e.g., Boatwright and Bundock, 2006; Daehne and Niemi, 2006).

This paper utilizes spatial intensity data and suggests a new approach to address the problem of locating the epicenter of historical earthquake. As a test case we use the 1927 Jericho earthquake, the second strongest instrumentally-recorded earthquake that occurred in Israel and its close vicinity (after the M7.1 of November 22, 1995).

2. Materials and methods

2.1. The 1927 Jericho earthquake

The 6.25 M_L July 11, 1927 Jericho earthquake was the most destructive earthquake in the 20th century in the vicinity of Israel (Avni, 1999). Estimations of casualties range between 250–500 death and 400–700 injuries (Amiran et al., 1994; Avni, 1999). Many buildings were damaged, landslides and rockfalls were observed along the Jerusalem–Jericho

* Corresponding author at: HaPisga 7, Kfar HaOranim 73134, Israel. Tel.: +972 8 9286925; fax: +972 72 2449606.
E-mail addresses: mottiz@mscc.huji.ac.il (M. Zohar), shmulikm@tau.ac.il (S. Marco).
[1] Present Affiliation: Department of Geography, the Hebrew University of Jerusalem, Mount Scopus, Jerusalem 91905, Israel and the Geological Survey of Israel, Jerusalem, Israel.

0926-9851/$ – see front matter © 2012 Elsevier B.V. All rights reserved.
doi:10.1016/j.jappgeo.2012.03.004

road and the flow of the Jordan River had stopped for 21.5 h. The towns of Nablus, Ramla, and Lod also suffered severe damage and casualties (Amiran et al., 1994; Avni, 1999; Avni et al., 2002). The location of the epicenter is controversial; while Ben Menahem et al. (1976) and Vered and Striem (1977) suggested a location near 'Damia' bridge (32.0ºN, 35.5ºE), Avni et al. (2002) identified erroneous interpretation of seismograms and suggested the location of 31.6ºN, 35.4ºE, some 50 km south and 10 km west of the previous estimate (Fig. 1). Estimates of the local magnitude given by Avni (1999), Ben Menahem et al. (1976) and Shapira (1979) are 6.25, 6.2 and 6.2 respectively.

This earthquake and many others in the region are associated with the activity of the Dead Sea Transform (DST) (Fig. 1), a left lateral fault between the Arabia plate and the sub-plate of Sinai (Garfunkel et al., 1981). The recent associated event had occurred in 11.02.2004 with an epicenter at the north of the Dead Sea and magnitude of 5.2 (Salamon, 2004).

2.2. Intensity data

We use intensity data evaluated by Avni (1999) as input (Appendix A). This dataset contains 133 localities attributed with mode, mean and max intensity values (MSK scale) based on a critical analysis of historical reports and evidence. The geographic distribution of the data spans between the Gulf of Aqaba in the south to the city of Zahle in the north, and from El-Arish in the west to Amman in the east (Fig. 2). However, the data do not include intensity evaluations in Iran, Iraq and Saudi Arabia due to political conditions (Avni, 1999). We also attempted to trace additional data through a search in the 'British National Archive' for activity logs of the 'Armoured Car Company No. 2' that was posted in the vicinity of Lod and Ramla during 1927. These logs may have provided additional information regarding medical aid given to casualties after the earthquake occurrence. Unfortunately, no records could be found.

3. Intensity corrections

Traditionally, the distance of a given locality from the epicenter is considered to be the dominant influence on the resulted damage, especially in cases of localities that are closer to the rupture (Bolt, 1978). At a far distance, however, the impact of the so-called 'site-attributes' increases. For instance, the cities of Lod, Ramla and Nablus (Fig. 1) that are located within a distance of 68, 64 and 82 km respectively from the epicenter calculated by Avni (1999), had suffered more damage than Jericho, which is only 25 km away from this presumed epicenter. This might imply that local amplification was dominant at these

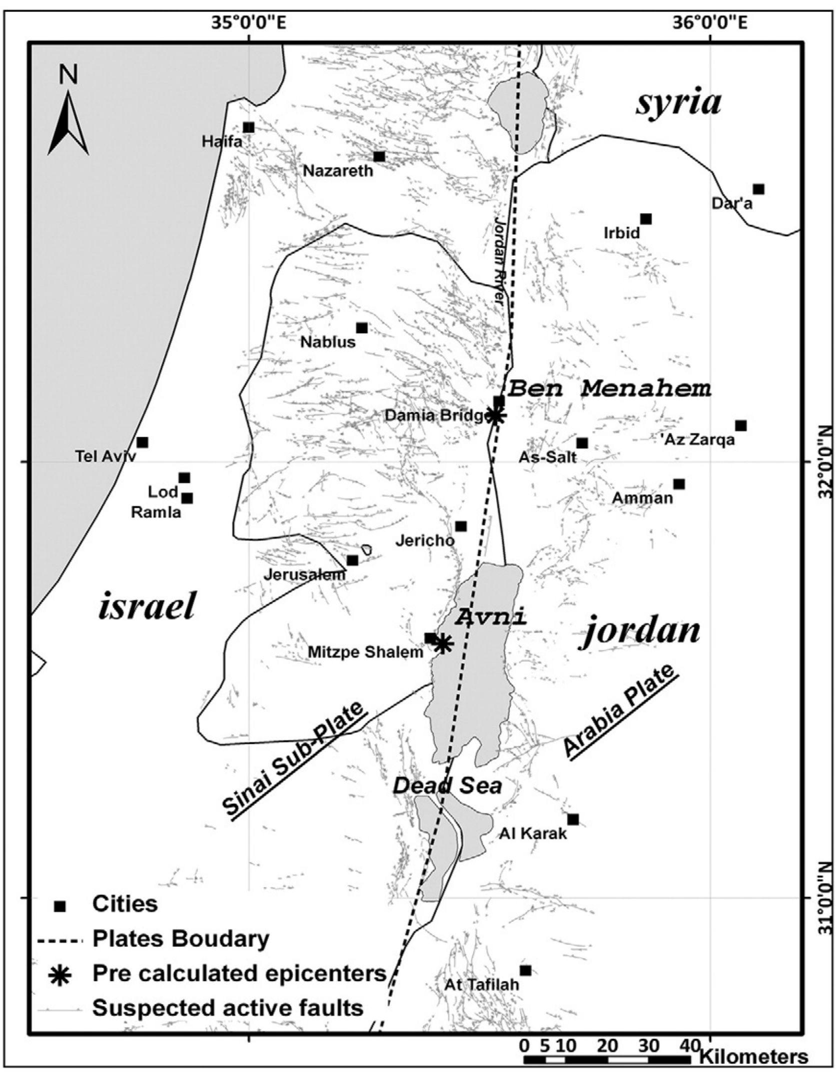

Fig. 1. The study area at the central Dead Sea Transform (DST) and suspected active faults (after Bartov et al., 2002). The map contains two previously suggested epicenters of the 6.25 M_L 1927 Jericho earthquake (marked in black asterisks): (1) Ben Menahem et al. (1976) and (2) Avni (1999) and Avni et al. (2002).

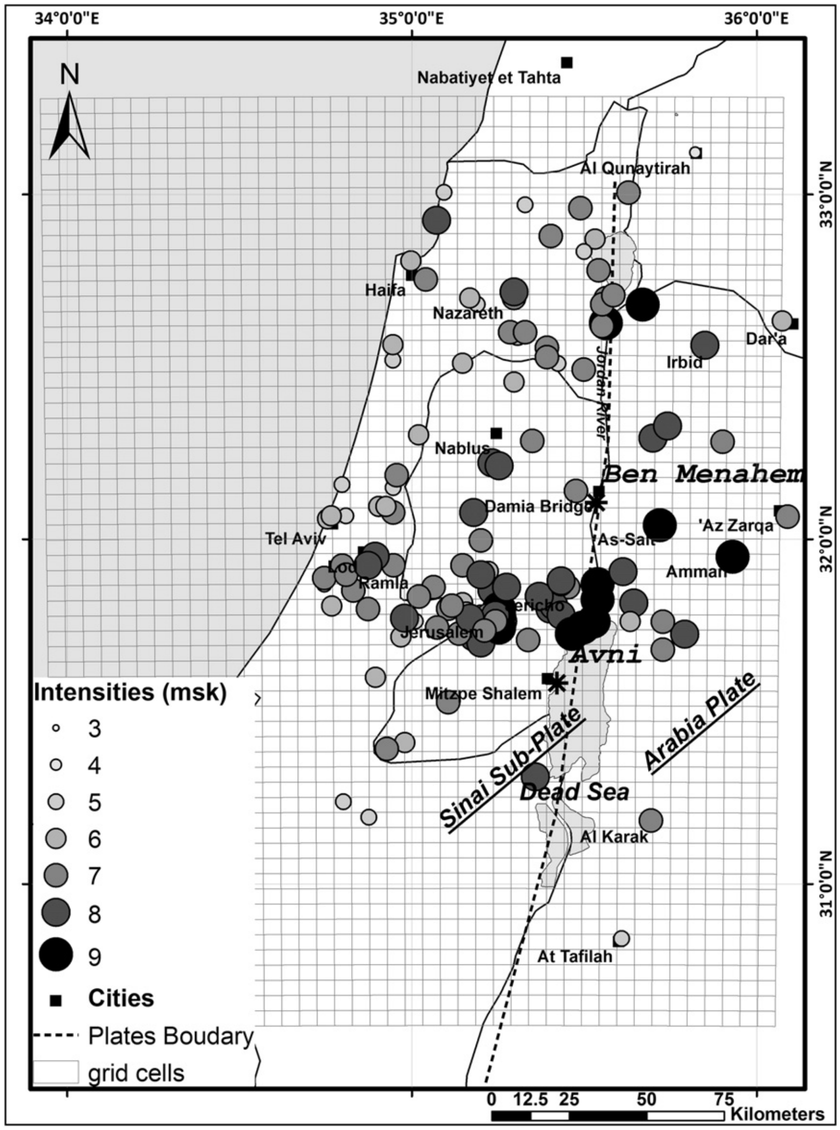

Fig. 2. The research area with depiction of (1) Spatial distribution of mode intensities evaluated by Avni, 1999, ranging from 3 to 9 in the MSK scale; (2) 5*5 km grid-cell structure representing 2501 assumed epicenters to be validated with the intensity data.

localities whereas attenuation was significant in Jericho. Following this insight, a preliminary stage of the analysis must consider the impact of site-attributes and correct the intensity value accordingly.

Being aware of the uncertainties involved with Intensity evaluation and quantification (Cecic and Musson, 2004), we categorize each of the inspected site-attributes and apply conservative thresholds in which beyond them, amplification or attenuation of the resulted damage most likely to occur.

Several site-attributes are considered:

(1) *Construction quality* – Equal ground acceleration will cause different damage to manmade structures depending on their material and construction (Bolt, 1978). In general, the quality of construction at the beginning of the 20th century is considered to be low and this is well described by Michaeli (1928) and Willis (1928), both experts that advised the government of necessary repairs after the earthquake. However, one could distinguish between two levels of construction quality. Towards the end of the 19th century, massive growth in Jewish population (Ben-Arieh, 1981) resulted establishments of new settlements (e.g., Tel Aviv, Petah Tiqwa) or expansion of existing such as Jerusalem and Haifa. These were built with contemporaneous new techniques and materials such as iron casting, cement and concrete (Fuchs, 1998; Krivoruchko, 1996) while Arabic settlements were less developed and were based primary upon pre 20th century traditional construction techniques, considered to be less resistant to shaking because of extensive use of raw materials such as adobe and wood. Accordingly, we classify localities into two groups of construction quality in which the Jewish settlements are considered stable (Table 1) and thus, ascribe exaggeration of intensities to the Arabic settlements.

(2) *Topographic slope* – the relation between damage and the underlying topographic slope is found to be significant (e.g., Athanasopoulos et al., 1988; Avni, 1999; Evernden et al., 1973; Wust-Bloch, 2002; Zaslavsky et al., 2000). Moreover, the larger the ratio between the height of the mountain peak above its surroundings to its width, the higher is the amplification (Salamon et al., 2010). Slope was calculated using a digital elevation model (DEM) of Hall and Cleave (1998) attributed with resolution of 25 m per pixel along with horizontal and vertical errors ranging between 10–50 m and less than 10 m

Table 1
The inspected site-attributes[a].

Site-attribute	*Sig. (1-tail)*	*Category*	*Description*	*Correction (in MSK units)*
Construction quality	0.005	1	Arab settlements – low standards of construction	−1
		2	Jewish settlements – high standards of construction	None
Topographic slope	0.000	1	0°–4.99°	None
		2	5°–14.99°	None
		3	15° and above	−1
Groundwater level depth	0.000	1	0–9.99 m	−1
		2	10–19.99 m	None
		3	20 m and above	None
Surface geology	0.016	1	Soft soils	None
		2	Soft materials (clay and marlstone)	None
		3	Rocks	+1
Population	0.147	1	Under 5000 people	Not corrected – factor is not significant
		2	5000 people and above	

[a] *Whereas Sig. (1-tail)* is the correlation significance of the given site-attribute with intensity, *Category* is the code classification (see also in Appendix A), *Description* is its characteristics and *Correction* represents the rate of correction in MSK units.

for 95% of the data respectively. Because the resolution is too low to use this DEM for calculating topographic slopes of individual structures, the slope of the area of each locality is calculated. Having a max slope value of 31°, we decided to use the median (15°) as a threshold of steep slope in which localities attributed with slope greater than this threshold are presumed to be overestimated (Table 1).

(3) *Groundwater level depth* – P and S waves behave differently as they pass through solid and liquid volumes. P waves travel trough both volumes, while the S waves travel only trough solid and tends to be absorbed in liquid (Bolt, 1978; Evernden et al., 1973). Researchers (e.g., Yang and Sato, 2000) found that depth of underground groundwater level, mainly in the manner of saturation and thickness, affects the movement of the ground in soft soils such as alluvial areas. Full analysis of this issue is rather complex and beyond the scope of our paper. Yet, we examine the groundwater level depth as a possible influencing factor. This is held using data of drills and bore holes collected in 1933/4 during a comprehensive survey throughout mandatory Palestine (Blake and Goldschmidt, 1947). Comparison of precipitation recorded in 1927 and 1933/4 enables to trace the fluctuation of groundwater level depth of the two sequences and estimate their 1927 contemporaneous depth. Nevertheless, accuracy of the data is limited and fraught with uncertainties whereas many of the localities are attributed with interpolated-based values. Furthermore, the 1933–4 groundwater level could have been influenced by the earthquake itself. Consequently, only intensity in localities with very shallow groundwater depth i.e., between 0 and 10 m (Table 1), were considered to be amplified.

(4) *Surface geology* – amplification occurs when there is a considerable decrease in shear wave velocity (Vs) toward the surface layers. Localities built on unconsolidated soils are likely to suffer more damage than those built on rocks (Yeats et al., 1997). Accordingly, we categorized localities into three surface geology classes (Table 1): (1) unconsolidated soil; (2) soft rock (clay and marlstone) and (3) solid rock, which tend to attenuate damage and thus, lead to underestimation of intensity.

(5) *Population* – Ambraseys (1971) found a correlation between density of populations to post-earthquake reports in which reports of densely populated area tend to be exaggerated. Feldman and Shapira (1994) found a tendency for higher estimation of seismic intensity in large cities such as Jerusalem and Tel Aviv. Consequently, we categorize localities into two classes defined by a population threshold of 5000 residents (Table 1).

To determine which of the site-attributes is significant, a multi-linear regression is carried out:

$$Y = \alpha_1{}^*X_1 + \alpha_2{}^*X_2 + \ldots\alpha_n{}^*X_n + \beta \tag{1}$$

Whereas Y is the mode intensity of a given locality, X_{1-n} represents a given site-attribute and α, β are the regression's slope and intercept respectively.

The significance of each site-attribute's correlation with intensity is listed in Table 1. Besides population, the correlation of all other four site-attributes with the intensity is found to be significant, meaning that we can reject the null hypothesis of no impact over the intensity. Accordingly, the population site-attribute was excluded from of the correction procedure.

Correction rate was set to the standard error of the mode intensity of (Avni, 1999). Being almost identical to one MSK unit (STD = 1.2419), the correction rate was refined accordingly to a value of 1 (Table 1) and is based upon linearity assumption that is, the difference between intensity 3 and 4 is identical as between 8 and 9. Out of 133 inspected localities, 111 were corrected.

4. Re-estimating the epicenter

Most of the seismic activity in the area is related to the Dead Sea Transform (DST) (Garfunkel et al., 1981). Thus, our inspected geographic area covers the central of DST region extending between 33.96° to 36.06° and 30.94° to 33.26° in the east–west and south–north axis respectively (Fig. 1). Initially, a set of assumed epicenters is generated and arranged in a 5*5 km grid-cell structure in which each polygon cell represents an assumed epicenter, totaling 2501 inspected cells (Fig. 2). Then we iterate these cells and calculate epicentral distances to the intensity localities (Fig. 3). However, the decay of intensity with distance is non linear and depends also on the azimuthal variations of the radiated energy (Howell and Schulz, 1975), anisotropic wave propagations (Stromeyer and Grunthal, 2009) and local site-effects (Bolt, 1978). Therefore, logarithmic proportionality (e.g., Bakun, 2006; Bakun and Scotti, 2006; Howell and Schulz, 1975; Stromeyer and Grunthal, 2009) is commonly used to describe this relationship. Following this approach, we adopt the attenuation relation developed by Stromeyer and Grunthal (2009) after Sponheuer (1960):

$$I = I^* - a\log\sqrt{\frac{R^2+h^2}{h^2}} - b\left(\sqrt{R^2+h^2} - h\right) \tag{2}$$

Where I is the given intensity, I^* is an estimate of the I_0 (Pasolini et al., 2008), a and b are constants representing the geometric spreading and absorption of energy respectively, R is the epicentral distance and h is the rupture depth. Assuming that I^*, a and b are constants, I depends on the following logarithmic proportionality:

$$I = \log\sqrt{\frac{R^2+h^2}{h^2}} - \left(\sqrt{R^2+h^2} - h\right) \tag{3}$$

Taking into consideration that most earthquakes that are related to the DST are generated in depth of up to 15 km (Shapira, 1979), h was set to 15 km and accordingly, a logarithmic factor for each of the epicentral distances calculated previously was generated.

Finally, for each cell we have correlated the intensities and their adjacent logarithmic factor of distance and use the 'Pearson' estimate as a quality indicator.

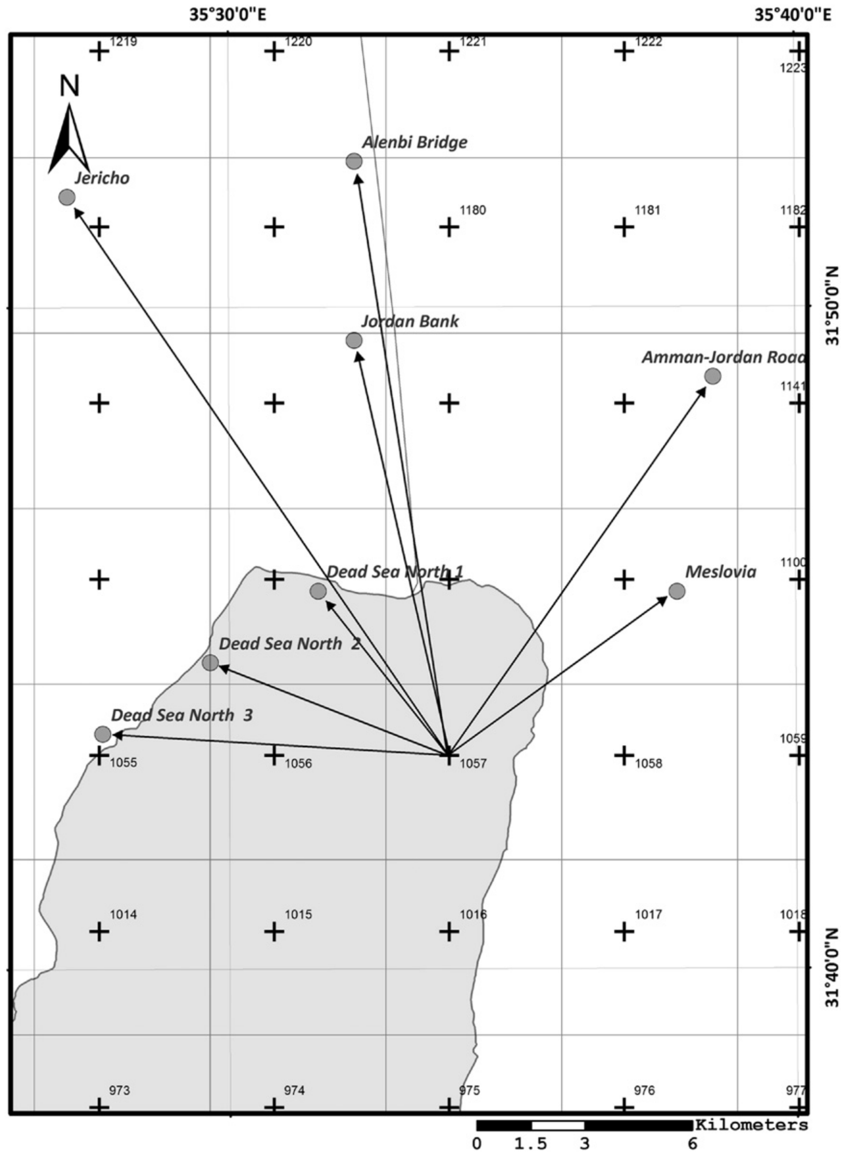

Fig. 3. Illustration of epicentral distances calculation for grid cell (assumed epicenter) 1057 to its surrounding intensities.

5. Results

Upon completeness of all 2501 cell correlations, we scaled and examined their Pearson indicators. These values range between 0.2061 and 0.6478 whereas the highest values are related to cells located at the north of the Dead Sea. Fig. 4 demonstrates a graduated colored grid in which each of its cells represents an adjacent Pearson indicator of an assumed epicenter. The highest correlation values, covering an area of approximately 50 km^2, are emphasized indicating the statistically most appropriate location of the epicenter. The center of mass of this area is located within the DST region and is about 35 km north of the epicenter calculated by Avni et al. (2002) and ~25 km south of the one calculated by Ben Menahem et al. (1976). Considering that the expected subsurface rupture length of such magnitude is approximately 20 km (Wells and Coppersmith, 1994), we conclude that this model is consistent with previous suggested locations with possible error of up to 50 km.

To demonstrate the importance of intensity correction we implement a similar model only with intensity data that was not corrected i.e., the raw mode intensity of Avni (1999). The result of this model is presented in Fig. 5 in which the suggested location is some 25 km east of the DST region. Furthermore, this indication is nearly 45 km north-east to Avni's calculation and 35 south-east of Ben-Menahem. That is, correction of the intensity yields a location that is more consistent with previous calculations than using uncorrected data.

Sensitivity of the model is also to be tested. This is done using exaggerated correction rate i.e., correcting the intensity with 2 MSK units instead of 1. The results are shown in Fig. 6 and demonstrate a location which is distant by far from the DST and the two previous calculations.

6. Discussion and conclusions

- The core of the process utilizes spatial distribution of intensities related to the 1927 Jericho earthquake. This is the first significant earthquake in the region for which we have both seismograph measurements and macroseimic data. Destructive earthquakes in the region had not occurred ever since and thus, the model could not be tested on additional local events.
- Though subjective and incomplete, the correction of intensities in accordance to local site-attributes is of great importance and in several cases, calibrates extreme intensities to their actual size. We concentrate in four site-attributes we find representatives of significance influence: construction quality, topographic slope, groundwater level

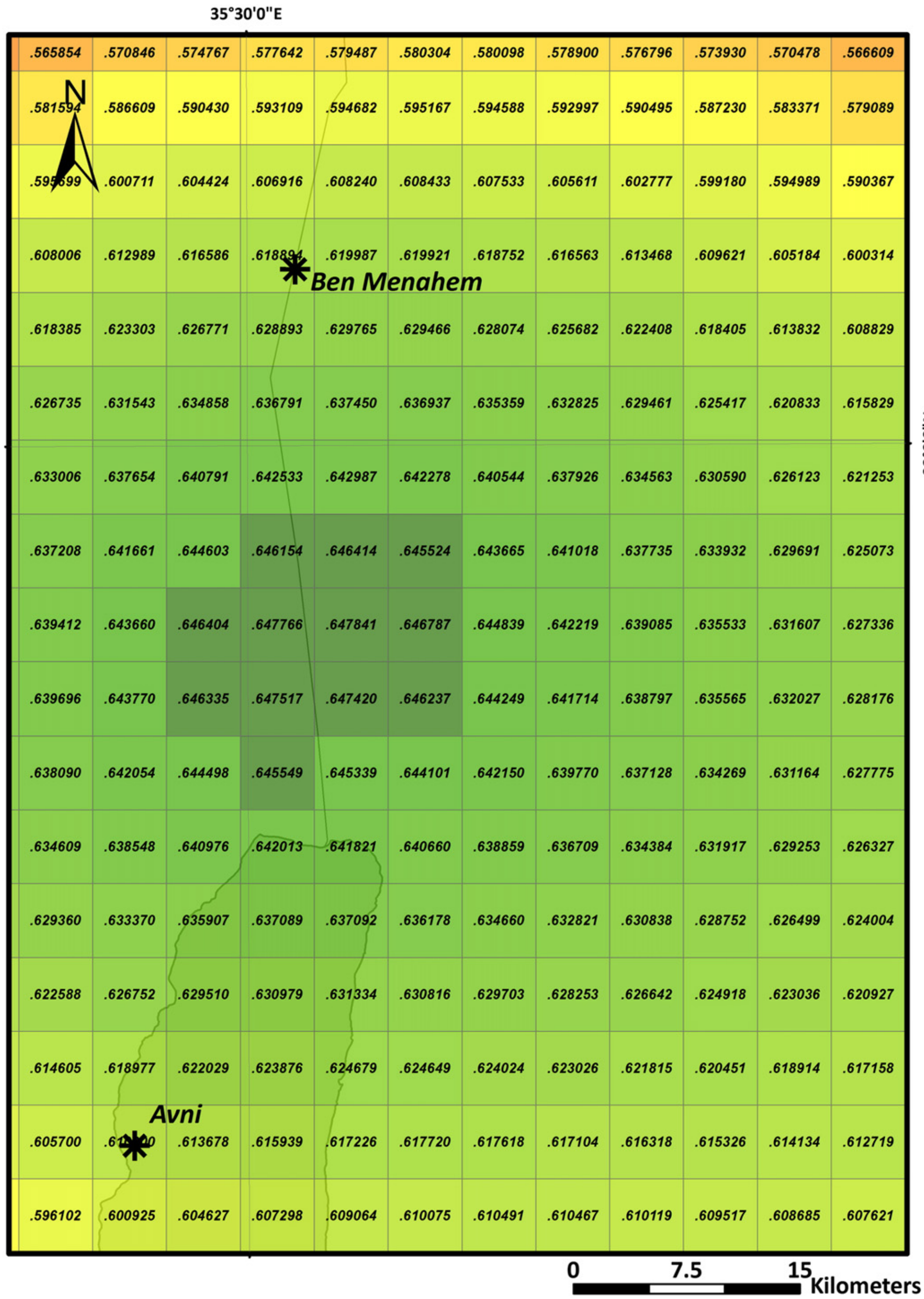

Fig. 4. Pearson correlation values of grid cells (assumed epicenters) correlated with corrected intensity data. Low values are colored in light red while high values are represented by dark green colors. A cluster of the highest values at the center of the figure represents the model preferred epicenter located between the two previously suggested epicenters of Avni et al. (2002) and Ben Menahem et al. (1976) (marked in black asterisks). (For interpretation of the references to color in this figure legend, the reader is referred to the web version of this article.)

depth and surface geology. Obviously, additional site-attributes could be added and thus improve the model accuracy.

- The MSK intensity scale we use is suited for European construction (mainly wood) whereas typical construction in the Levant area includes also soft material such as mud and bricks. Furthermore, there is a difference between the two regions in which surface geology and ground soils respond differently to ground shaking (Ramazi and Haghani, 2007). Nevertheless, we use the European scale for two reasons: (1) there is no other scale suited specifically for the Levant and the MSK scale is the most similar, and (2) errors that occur in estimating the intensity values will probably reflect most localities equally, and will not affect dramatically on the epicenter location.
- The result of the proposed method coincides with the seismogram-based calculation of Avni (1999) and also of Ben Menahem et al. (1976) with spatial error of 50 km. However, it is not aimed at

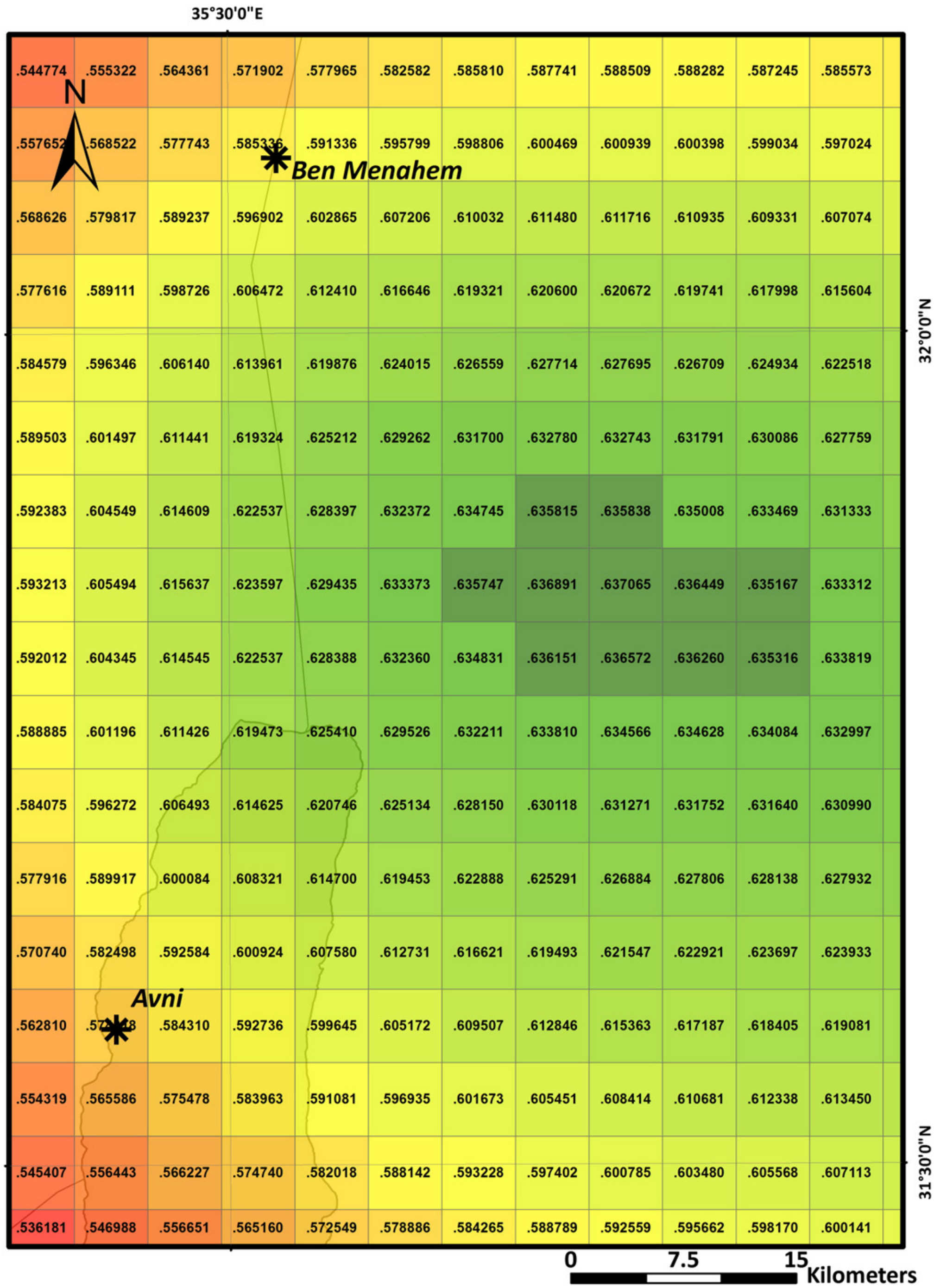

Fig. 5. Pearson correlation values of grid cells (assumed epicenters) correlated with raw intensity data that was not corrected. Low values are colored in light red while high values are represented by dark green colors. A cluster of the highest values is emphasized at the right edge of the figure representing the model suggestion for the epicenter. This location is some 25 km east of the DST region and is less consistent with the two previously suggested of Avni et al. (2002) and Ben Menahem et al. (1976) (marked in black asterisks).

distinguishing between these former calculations; rather, it provides an additional method for estimating the earthquake epicenter.

Acknowledgements

We thank Prof. Izhak Bennenson, the Geography department at Tel Aviv University and Dr. Ron Avni from Ben Gurion University for their guidance and advice. We also thank Dr. Amichai Sneh, Dr. John Hall, and Mr. Hayim Hemo of the Geological Survey of Israel for providing data. We highly appreciate the constructive reviews by an anonymous journal referee and by Prof. Jeremy Zechar, which significantly improved the manuscript. Finally, we thank the Geological Survey of Israel and the Department of Geography at the Hebrew University for providing supportive environment. The research was partly funded by the Israel Science Foundation grant #12/2003 to S. Marco.

Appendix A. Database of the research

Description of fields and their adjacent abbreviations (in brackets): (1) Sequential id of localities (ID); (2) locality name (Name); (3) Longitude in Decimal Degrees (Lon); (4) Latitude Decimal Degrees (Lat); (5) Mode intensity (Md); (6) Mean intensity (Mn); (7) Number of observations for mean intensity (N.Mn); (8) Max intensity (Mx); (9) Construction quality category (Con.C);

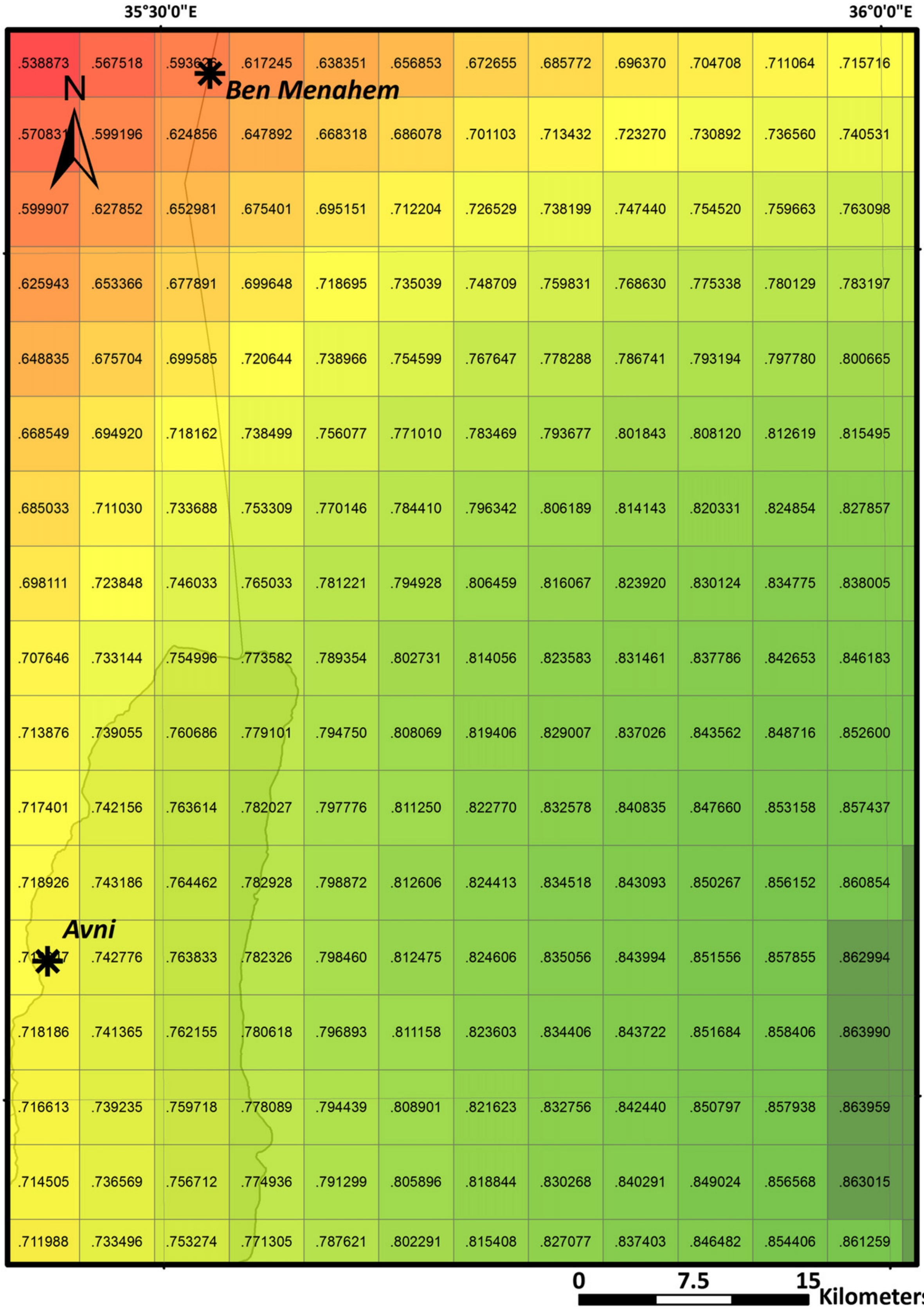

Fig. 6. Pearson correlation values of grid cells (assumed epicenters) correlated with exaggerated corrected intensity data. Low values are colored in light red while high values are represented by dark green colors. A cluster of the highest values is emphasized at the right edge of the figure representing the model suggestion for the epicenter. This location is some 60 km east of the DST region and by far distant from the two previously suggested epicenters of Avni et al. (2002) and Ben Menahem et al. (1976) (marked in black asterisks).

(10) Slope (in degrees) (Slp); (11) Slope category (Slp.C); (12) Groundwater level (in meters) (Wat); (13) Groundwater level category (Wat.C); (14) Surface geology category (Geo.C); (15) Population (Pop); (16) Population category (Pop.C); (17) Corrected mode intensity using a rate of 1 MSK unit (C1.Md); (18) Corrected mode intensity using a rate of 2 MSK units (C2.Md); *fields 5–8 contain raw intensity data and field 15 contain the 1927 population following Avni (1999).

ID	Name	Lon	Lat	Md*	Mn*	N.Mn*	Mx*	Con.C	Slp	Slp.C	Wat	Wat.C	Geo.C	Pop*	Pop.C	C1.Md	C2.Md
1	Abu-Gosh	35.104	31.798	6.5	6.5	10	6.5	1			70	4	3		1	6.5	6.5
2	Abu-Dis	35.263	31.762	8	7.5	11	8	1			80	4	3	1178	1	8	8
3	Abu-Tlul	34.874	31.194	5	5	2	5	1			44	4	3		1	5	5
4	Um-el-Fahm	35.146	32.511	5.5	5.5	1	5.5	1			12	2	3		1	5.5	5.5
5	Um Juni	35.562	32.700	6.5	7	7	6.5	1					1		1	5.5	4.5
6	El Hama	35.658	32.681	6.5	7	5	6.5	1					3		1	6.5	6.5
7	El Arish	33.755	31.152	4.5	4.5	1	4.5	1					1		1	3.5	2.5
8	Alexandria	29.897	31.203	3	3	1	3	1					1		1	2	1
9	A-Salt	35.718	32.041	8.5	8.5	1	8.5	1					3		1	8.5	8.5
10	Irbid	35.849	32.563	7.5	7.5	1	7.5	1					2		1	6.5	5.5
11	A-Ram	35.231	31.852	8	7	13	8.5	1			80	4	3	238	1	8	8
12	Beer Sheva	34.800	31.238	5	5	2	5	2			56	4	1	2691	1	5	5
13	Bira	35.220	31.907	6	7.5	5	6	1			78	4	3		1	6	6
14	Bet Alfa	35.423	32.511	5	6	4	5	2			32	3	1		1	5	5
15	Bet Jala	35.178	31.717	7.5	7.5	12	7.5	1			78	4	3	2895	1	7.5	7.5
16	Bet Govrin	34.894	31.600	6	6	1	6	2	6	2	43	4	3	1633	1	7	8
17	Bet Gimal	34.967	31.717	6	6.5	4	6	1	7	2	52	4	3	120	1	6	6
18	Bet HaKerem	35.199	31.780	5.5	7	16	5.5	2	4	1	80	4	3	369	1	6.5	7.5
19	Bet Lehem	35.199	31.699	8	7.5	10	8	1	11	2	79	4	3	6745	2	8	8
20	Bet Likia	35.062	31.861	7	6.5	5	7	1	9	2	61	4	3	805	1	7	7
21	Bet Shean	35.497	32.492	6.5	6	2	6.5	2	0	1	41	4	2		1	6.5	6.5
22	Bet Sorik	35.146	31.816	6	7	11	6	1	18	3	76	4	3	396	1	5	4
23	Binyamina	34.944	32.519	5	5.5	2	5	2	1	1	9	1	1	729	1	4	3
24	Batir	35.136	31.726	7	7	11	7	1	14	2	72	4	2	664	1	6	5
25	Gedera	34.766	31.807	5.5	6	4	5.5	2	3	1	37	3	3		1	6.5	7.5
26	Gimzoo	34.945	31.924	7	7.5	4	7	2	6	2	48	4	3	999	1	8	9
27	Jiftlik	35.475	32.141	7	7	1	7	1	11	2	49	4	1		1	6	5
28	Jaljulia	34.945	32.150	4.5	6	5	4.5	1	0	1	25	3	1	199	1	3.5	2.5
29	Genin	35.295	32.457	6	6	1	6	1	11	2	24	3	3	2713	1	6	6
30	Jeser Magmi	35.561	32.627	8.5	7	6	8.5	1	1	1			1	232	1	7.5	6.5
31	Jeresh	35.900	32.283	7	7	1	7	1	2	1			3		1	7	7
32	Gesher	35.551	32.618	6.5	7	5	6.5	2	7	2			1		1	6.5	6.5
33	Alenbi Bridge	35.537	31.870	8.5	8	5	9	2	1	1			2		1	8.5	8.5
34	Bnot – Yaa'kov	35.627	33.006	6.5	6.5	1	6.5	2	12	2			2		1	6.5	6.5
35	Daharia	34.978	31.410	5.5	6	2	5.5	1	18	3	43	4	3	2635	1	4.5	3.5
36	Dir-a-Shech	35.073	31.744	6.5	6.5	9	7	1	13	2	66	4	3		1	6.5	6.5
37	Demaskus	36.297	33.516	4.5	4.5	1	4.5	1					0		1	3.5	2.5
38	Daraa'	36.073	32.634	6	6	1	6	1	3	1			0		1	5	4
39	Zeitim Mountain	35.252	31.780	8.5	7.5	14	9	1	18	3	80	4	3		1	7.5	6.5
40	Toov Mountain	35.009	31.762	5	6.5	5	5	2	2	1	57	4	2		1	5	5
41	Carmel Mountain	35.039	32.754	6.5	6	2	6.5	2	19	3	10	1	3		1	5.5	4.5
42	Zofim Mountain	35.252	31.798	8.5	7.5	13	8.5	2	16	3	80	4	1		1	7.5	6.5
43	Herzelia	34.796	32.158	5	5	1	5	2	2	1	24	3	1		1	5	5
44	Vadi Shueib	35.611	31.906	8	8	2	8	1	1	1			1		1	7	6
45	Zarka	36.089	32.066	7	7	1	7	1	1	1			0		1	6	5
46	Zichron Yaa'kov	34.944	32.565	6	5.5	2	6	2	5	2	9	1	2	1373	1	5	4
47	Zarka Maein	35.727	31.680	7	7.5	2	7	1	0	1			2		1	6	5
48	Hebron	35.104	31.528	7	7	1	8	1	22	3	55	4	3	17107	2	6	5
49	Haifa	34.996	32.808	6	6	2	7	2	16	3	12	2	3	38995	2	6	6
50	Tabha	35.530	32.871	6	6.5	2	6	1	8	2			3		1	6	6
51	Tiberias	35.541	32.781	7	6.5	2	7	2	11	2			1	8069	2	7	7
52	Tool-Karem	35.019	32.303	6	6	1	6	1	1	1	41	4	3	4471	1	6	6
53	Tapila	35.607	30.842	5	5	1	5	1	11	2			3		1	5	5
54	Yalo	35.020	31.834	7	7	7	7	1	6	2	57	4	2	895	1	6	5
55	Yavne	34.745	31.870	5	6	5	5	2	2	1	29	3	1		1	5	5
56	Jafa	34.754	32.059	6	5.5	3	6	1	1	1	24	3	1	44603	2	5	4
57	Jerusalem	35.220	31.780	7	7	250	8.5	1	4	1			3	78092	2	7	7
58	Armon-HaNatziv	35.252	31.744	8.5	7.5	12	8.5	2	11	2	80	4	3		1	9.5	10.5
59	Holly Mountain	35.241	31.780	7.5	7.5	15	7.5	1	12	2	80	4	3		1	7.5	7.5
60	Jericho	35.453	31.861	7	8	10	8	1	1	1	74	4	1	1548	1	6	5
61	Jru. – Jericho Road 1	35.400	31.798	8	8	8	8	1	16	3	79	4	3		1	7	6
62	Jre. – Jericho Road 2	35.410	31.807	8	7.5	7	8	1	14	2	79	4	3		1	8	8
63	Amman – Jordan Road	35.643	31.816	8	8	4	8	1	2	1			1		1	7	6
64	Michmach Village	35.273	31.861	8	7.5	6	8	1	18	3	83	4	3		1	7	6
65	Shiloach Village	35.241	31.762	7	7.5	14	7.5	2	14	2	79	4	3		1	8	9
66	Kafaringi	35.698	32.293	8	8	2	8	1	12	2			3		1	8	8
67	Karach	35.692	31.184	6.5	6.5	1	6.5	1	15	3			3		1	5.5	4.5
68	Lod	34.892	31.951	8	7	6	8	1	0	1	43	4	1	9851	2	7	6
69	Migdal	35.498	32.835	5	5	1	5	2	9	2	35	3	1	248	1	5	5
70	Migdal Yava	34.945	32.078	6.5	5.5	4	6.5	2	0	1	28	3	3	859	1	7.5	8.5
71	Midba	35.790	31.725	7.5	7	3	7.5	1	6	2			2		1	6.5	5.5

(continued on next page)

Appendix A (*continued*)

ID	Name	Lon	Lat	Md*	Mn*	N.Mn*	Mx*	Con.C	Slp	Slp.C	Wat	Wat.C	Geo.C	Pop*	Pop.C	C1.Md	C2.Md
72	Moza	35.157	31.789	6	7.5	16	6	2	5	2	78	4	3		1	7	8
73	Maa'n	35.717	30.188	5	5	1	5	1					0		1	4	3
74	Maa'yan Elisha	35.432	31.870	7	7.5	7	7	2	20	3	78	4	1		1	6	5
75	Mrar	35.402	32.880	7	7	1	7	1	4	1	24	2	3		1	7	7
76	Masada	35.357	31.311	8	8	1	8	1	18	3	51	4	2		1	6	4
77	Merhavia	35.306	32.592	6	6.5	4	6	2	0	1	17	2	1		1	6	6
78	Mar-sava	35.336	31.708	6.5	7.5	3	6.5	1	5	2	75	4	3		1	6.5	6.5
79	Meslovia	35.632	31.761	6	8	4	6	1	7	2			1		1	5	4
80	Nabi – Musa	35.431	31.780	7.5	8	7	7.5	1	15	2	75	4	3		1	7.5	7.5
81	Nahalal	35.188	32.682	4.5	6	3	4.5	2	1	1	13	2	2	409	1	4.5	4.5
82	Naharia	35.092	33.007	4.5	6	2	4.5	2	1	1	4	1	1		1	3.5	2.5
83	Sorek River	34.872	31.798	7	6.5	5	7	2	2	1	44	4	1		1	7	7
84	Nes-Ziona	34.797	31.924	6.5	7	5	6.5	2	0	1	31	3	1		1	6.5	6.5
85	Nazeret	35.295	32.700	7	7	4	7.5	1	11	2	14	2	3	8241	2	7	7
86	Salfit	35.178	32.078	7.5	7	2	7.5	1	17	3	53	4	2		1	5.5	3.5
87	Sweida	36.575	32.702	7	7	1	7	1					0		1	6	5
88	Abadia	35.551	32.682	7	7	6	7	1	4	1			1		1	6	5
89	Ajloon	35.741	32.329	8	8	2	8	1	13	2			3		1	8	8
90	Gaza	34.462	31.499	6.5	6.5	1	7	1	0	1	53	4	1		1	5.5	4.5
91	Azraa'	36.235	32.849	6	6	1	6	1					0		1	5	4
92	Atara	35.199	31.997	7	7	4	7	1	7	2	57	4	3	180	1	7	7
93	Ein-el-Kelt	35.368	31.834	8	7.5	9	8	1	16	3	84	4	3		1	7	6
94	Ein Dok	35.432	31.879	8	7.5	7	8	1	33	3	78	4	1		1	6	4
95	Ein Harod	35.391	32.556	6.5	6	5	6.5	2	4	1	27	3	1	377	1	6.5	6.5
96	Ein Karem	35.168	31.771	7.5	7	18	7.5	1	17	3	79	4	3		1	6.5	5.5
97	Ein Musa	35.727	31.761	7	7	3	7	1	17	3			0		1	5	3
98	Ein Kinia	35.146	31.925	7	7	5	7	1	13	2	66	4	3	71	1	7	7
99	Ein Fara'	35.348	32.285	7	7	1	7	1	6	2	47	4	3		1	7	7
100	Aco	35.071	32.925	7.5	6	2	8	1	2	1	6	1	1	7389	2	5.5	3.5
101	Anab	34.926	31.392	6.5	6	2	6.5	1	8	2	45	4	3		1	6.5	6.5
102	Afula	35.284	32.601	7	6.5	4	7	2	0	1	14	2	2		1	7	7
103	Akaba	35.003	29.534	4	4	1	4	1	0	1			1		1	3	2
104	Ekron	34.829	31.852	6.5	6.5	7	6.5	2	1	1	36	3	1	335	1	6.5	6.5
105	Pki'in	35.327	32.971	4.5	4.5	1	4.5	2	8	2	14	2	3		1	5.5	6.5
106	Petah Tikva	34.903	32.096	5.5	5.5	5	6	2	0	1	23	3	1	5247	2	5.5	5.5
107	Tzemach	35.583	32.709	7	7	7	7	2	1	1			1		1	7	7
108	Safed	35.488	32.961	6.5	6.5	1	6.5	2	18	3	24	3	3	9139	2	6.5	6.5
109	Tzora	34.978	31.771	8	6.5	5	8	2	14	2	53	4	3		1	9	10
110	Kabab	34.745	31.888	7	7	7	7	1	0	1	28	3	1	1401	1	6	5
111	Cairo	31.201	30.040	3.5	3.5	1	3.5	1					0		1	2.5	1.5
112	Kunetra	35.821	33.122	4	4	1	4	1	0	1			1		1	3	2
113	Kalkilia	34.955	32.186	6.5	5.5	3	6.5	1	1	1	32	3	1	3394	1	5.5	4.5
114	Kiriat Anavim	35.115	31.807	7	7	11	7	2	10	2	70	4	3		1	8	9
115	Rammala	35.199	31.897	7.5	7.5	5	7.5	1	12	2	75	4	3	3761	1	7.5	7.5
116	Rosh Ha'ayin	34.924	32.096	6	6	5	6	2	0	1	24	3	1		1	6	6
117	Amman	35.929	31.950	8.5	8.5	1	9	1	1	1			3		1	8.5	8.5
118	Rehovot	34.808	31.897	6.5	6.5	6	6.5	2	3	1	33	3	1		1	6.5	6.5
119	Reina	35.295	32.718	8	7.5	2	8	1	16	3	16	2	3		1	7	6
120	Ramle	34.871	31.924	8	7	7	8	1	0	1	45	4	1	8998	2	7	6
121	Ramat Yishai	35.167	32.700	6	5	2	6	2	4	1	14	2	2		1	6	6
122	Ramat Rachel	35.210	31.735	6.5	7.5	14	6.5	2	9	2	83	4	3		1	7.5	8.5
123	Refidie	35.231	32.222	8	8	2	8	1	15	3	44	4	3	392	1	7	6
124	Shunam	35.327	32.601	7	6.5	5	7	1	2	1	20	2	1		1	6	5
125	Borochov Nei.	34.807	32.068	5	5.5	4	5	2	5	2	25	3	1		1	5	5
126	Nablus	35.252	32.213	8	8	2	8.5	1	19	3	45	4	3	16809	2	7	6
127	Tel Aviv	34.765	32.068	6	5.5	3	6	2	1	1			1	32349	2	6	6
128	Tel Yosef	35.391	32.529	6.5	6	3	6.5	2	22	3	29	3	1	195	1	5.5	4.5
129	Dead sea North 1	35.526	31.762	9	8.5	4	9	1	5	2			1		1	8	7
130	Dead sea North 2	35.463	31.726	9	8.5	4	9	1	1	1	72	4	1		1	8	7
131	Dead sea North 3	35.495	31.744	9	8.5	4	9	1	6	3	66	4	1		1	7	5
132	Jordan Bank	35.537	31.825	9	8.5	6	9	1	3	1			2		1	8	7
133	Yarmuch fall	35.668	32.681	8.5	7	4	8.5	1	17	3			3		1	7.5	6.5

References

Ambraseys, N.N., 1971. Value of Historical Records of Earthquakes. Nature 232, 375–379.

Ambraseys, N.N., 2005. Historical earthquakes in Jerusalem - A methodological discussion. Journal of Seismology 9, 329–340.

Ambraseys, N.N., 2009. Earthquakes in the Mediterranean and Middle East. A Multidisciplinary Study of Seismicity up to 1900 (1 ed.). New York: Cambridge University. Press.

Ambraseys, N.N., Melville, C.P., Adams, R.D., 1994. The Seismicity of Egypt, Arabia and the Red Sea: A Historical Review. Cambridge, UK.

Amiran, D.H.K., Arieh, E., Turcotte, T., 1994. Earthquakes in Israel and adjacent areas: Macroseismic observation since 100 B.C.E. Israel exploration Journal 44 (3–4), 260–305.

Athanasopoulos, G.A., Pelekis, P.C., Leonidou, E.A., 1988. Effects of surface topography on seismic ground response in the Egion (Greece) 15 June 1995 earthquake. Soil Dynamics and Earthquake Engineering 18, 135–149.

Avni, R., 1999. The 1927 Jericho Earthquake. Comprehensive Macroseismic Analysis Based on Contemporary Sources. Ben Gurion University of the Negev, Beer Sheva (in Hebrew).

Avni, R., Bowman, D., Shapira, A., Nur, A., 2002. Erroneous interpretation of historical documents related to the epicenter of the 1927 Jericho earthquake in the Holy Land. Journal of Seismology 6, 469–476.

Bakun, H.W., 2006. Estimating Locations and Magnitudes of earthquakes in Southern california from Modified Mercalli Intensities. Bulletin of the Seismological Society of America 96, 1278–1295.

Bakun, H.W., Wentworth, C.M., 1997. Estimating earthquake location and Magnitude from Seismic Intensity Data. Bulletin of the Seismological Society of America 87 (6), 1502–1521.

Bakun, H.W., Scotti, O., 2006. Regional intensity attenuation models for France and the estimation of magnitude and location of historical earthquakes. Geophysical Journal International 164, 596–610.

Bakun, H.W., Johnston, A.C., Hopper, M.G., 2003. Estimating locations and magnitudes of earthquakes in eastern North America from Modified Mercalli intensities. Bulletin of the Seismological Society of America 93 (1), 190–202.

Bartov, Y., Sneh, A., Fleischer, L., Arad, V., Rosensaft, M., 2002. Suspected active faults in Israel, 1:200000. The Geological Survey of Israel.

Ben Menahem, A., Nur, A., Vered, M., 1976. Tectonics, seismicity and structure of the Afro-Eurasian junction–the breaking of the incoherent plate. Physics of the Earth and Planetary Interiors 12, 1–50.

Ben-Arieh, Y., 1981. The twelve large settlements in Eretz Israel in the 19th century. Cathedra 19, 83–143 (in Hebrew).

Blake, G.S., Goldschmidt, M.J., 1947. Geology and Water Resources of Palestine. Goverment of Palestine, Jerusalem. 471 pp.

Boatwright, J., Bundock, H., 2006. Re-evaluating the Intensity Distribution of the 1906 San Francisco Earthquake. In: Survey, U.G. (Ed.), Centennial Meeting of the Seismological Society of America: San Francisco, California, USA.

Bolt, A., 1978. Earthquakes. W. H. Freeman & company, New York. 318 pp.

Cecic, I., Musson, R., 2004. Macroseismic surveys in theory and practice. Natural Hazards 31, 39–61.

Daehne, A., Niemi, D., 2006. Using the Lawson Report and Other Historical Documents to Investigate Fault Morphology and Coseismic Slip of the 1906 Earthquake in Marin County. Centennial Meeting of the Seismological Society of America: San Francisco, California, USA.

Evernden, J.F., Hibbard, R.R., Schneider, J.F., 1973. Interpretation of seismic intensity data. Bulletin of the Seismological Society of America 63, 399–433.

Feldman, L., Shapira, A., 1994. Analysis of seismic intensities observed in Israel. Natural Hazards 9, 287–301.

Fuchs, R., 1998. The Palestinian Arab House Reconsidered. Part 2: Domestic Architecture in the 19th Century. Cathedra 90, 53–86.

Garfunkel, Z., Zak, I., Freund, R., 1981. Active faulting in the Dead Sea rift. Tectonophysics 80, 1–26.

Gasperini, P., Vannucci, G., Tripone, D., Boschi, E., 2010. The Location and Sizing of Historical Earthquakes Using the Attenuation of Macroseismic Intensity with Distance. Bulletin of the Seismological Society of America 100 (5A), 2035–2066.

Grünthal, G., 1998. European Macroseismic Scale 1998 EMS-98. European Seismological Commission, Luxembourg.

Guidoboni, E., Comastri, A., 2005. Catalogue of earthquakes and tsunamies in the Mediterranean area from the 11th to the 15th century. Bologna: INGV-GA.

Guidoboni, E., Comastri, A., Traina, G., 1994. Catalogue of ancient earthquakes in the Mediterranean area up to the 10th Century. Bologna, Italy: ING-GA.

Hall, J.K., Cleave, R.L., 1998. The DTM project. Geological Survey of Israel 6, 1–7.

Howell, B.F., Schulz, T.R., 1975. Attenuation of modified Mercalli intensity with distance from the epicenter. Bulletin of the Seismological Society of America 65, 651–665.

Johnston, K., Ver Hoef, M.J., Krivoruchko, K., Lucas, N., 2001. Using ArcGis Geostatistical Analysis. ESRI press.

Karcz, I., Lom, P., 1987. Bibliographic reliability of catalogues of historic earthquakes in and around Israel. Jerusalem: Geological Survey of Israel.

Krivoruchko, K., 1996. Jerusalem architecture: Jerusalem. Keter Publishing House.

Medvedev, S.W., Sponheuer, W., Karnik, V., 1965. Seismic Intensity Scale version MSK 1964. United nation educational, scientific and cultural organization, Paris, p. 7.

Michaeli, C.E., 1928. Notes on the Earthquake. Construction and Industry 11–12, 9–12.

Michetti, A.M., Esposito, E., Gürpinar, A., Mohammadioun, J., Mohammadioun, B., Porfido, S., et al., 2004. The Inqua scale; an innovative approach for assessing earthquake intensities based on seismically-induced ground effects in natural environment: Servizio Geologico d'Italia, Dipartimento Difesa del Suolo, Agenzia per la Protezione dell'ambiente e per i Servizi Tecnici (APAT), Rome, Italy.

Pasolini, C., Gasparini, P., Albarello, D., Lolli, B., D'Amico, V., 2008. The attenuation of seismic intensity in Italy, part 1: Theoretical and empirical backgrounds. Bulletin of the Seismological Society of America 98, 682–691.

Ramazi, H., Haghani, R., 2007. New criteria for an intensity scale in Iran and surrounding countries. Seismological Research Letters 78, 422–428.

Salamon, A., 2004. Seismically induced ground effects of the February 11, 2004, ML=5.2, northeastern Dead Sea earthquake. Geological Survey of Israel, Jerusalem.

Salamon, A., Katz, O., Crouvi, O., 2010. Zones of required investigation for earthquake-related hazards in Jerusalem. Natural Hazards 53, 375–406.

Sbeinati, M.R., Darawcheh, R., Mouty, M., 2005. The historical earthquakes of Syria: an analysis of large and moderate earthquakes from 1365 B.C. to 1900 A.D. Annals of Geophysics 47, 733–758.

Shapira, A., 1979. Re-Determined Magnitude of Earthquakes in the Afro-Euroasian Junction. Israel Journal of Earth Sciences 28, 107–109.

Sirovich, L., 1996. A Simple Algorithm for Tracing Synthetic Isoseismals. Bulletin of the Seismological Society of America 86 (4), 1019–1027.

Sirovich, L., Pettenati, F., 2001. Test of Source-Parameter Inversion of the intensities of a 54,000-Death Shock of the Seventeenth Century in Southeast Sicily. Bulletin of the Seismological Society of America 91 (4), 792–811.

Sirovich, L., Pettenati, F., Chiaruttini, C., 2001. Test of Source-Parameter Inversion of Intensity Data. Natural Hazards 24, 105–131.

Sponheuer, W., 1960. Methoden zur Herdtiefenbestimmung in der Makroseismik. Freiberger Forschungshefte C88. Akademie Verlag, Berlin.

Stromeyer, D., Grunthal, G., 2009. Attenuation Relationship of Macroseismic Intensities in Central Europe. Bulletin of the Seismological Society of America 99, 554–565.

Vered, M., Striem, H.L., 1977. A macroseismic study and the implications of structural damage of two recent major earthquakes in the Jordan rift. Bulletin of the Seismological Society of America 67, 1607–1613.

Wells, D.L., Coppersmith, K.J., 1994. New empirical relationships among magnitude, rupture length, rupture width, rupture area, and surface displacement. Bulletin Of The Seismological Society Of America 84, 974–1002.

Willis, B., 1928. Earthquakes in the holy land. Bulletin of the seismological society of America 18, 72–103.

Wood, H.O., Neumann, F., 1931. Modified Mercalli Intensity Scale of 1931. Bulletin of the Seismological Society of America 21, 277–283.

Wust-Bloch, G.H., 2002. The Active Dead Sea Rift fault zone: a seismic wave-guide. EGU Stephan Mueller Publication Series 2, 11–20.

Yang, J., Sato, T., 2000. Interpretation of seismic vertical amplification observed at an array site. Bulletin of the Seismological Society of America 90, 275–285.

Yeats, S.R., Sieh, K., Allen, R.C., 1997. The Geology of Earthquakes. Oxford university press, Inc., New York. 557 pp.

Zaslavsky, Y., Shapira, A., Arzi, A.A., 2000. Amplification effects from earthquakes and ambient noise in the Dead Sea rift (Israel). Soil Dynamics and Earthquake Engineering 20 (1–4), 187–207.